Journal of Non-Crystalline Solids 583 (2022) 121474

Contents lists available at ScienceDirect

Journal of Non-Crystalline Solids

journal homepage: www.elsevier.com/locate/jnoncrysol

Effect of Lithium Iodide on transport phenomenon in Lithium Borophosphate glass Electrolyte

V.A. Adhwaryu [a], D.K. Kanchan [b,c,*]

[a] Department of Science and Humanities, L. D. College OF Engineering, Ahmedabad, 380015, Gujarat, India
[b] Solid State Ionics and Glass research lab, Department of Physics, The M.S. University of Baroda, Vadodara, 390 002, Gujarat, India
[c] Presently working at: ITM(SLS) BARODA UNIVERSITY, Jarod, Vadodara, 391510, Gujarat, India

ARTICLE INFO

Keywords:
Lithium Borophosphate glass
Jonscher's power law (JPL)
Enthalpy ($H_m + H_f$)
Correlated Barrier Hopping (CBH) model
Polaron binding energy (U_M)
Coulombic (effective) barrier height (U_H)

ABSTRACT

Ion transport study for the lithium iodide doped Lithium Borophosphate (LBP) glass electrolyte $x(LiI) : [(100-x).(60Li_2O : 8B_2O_3 : 32P_2O_5)]$ has been carried out over a range of composition (x=0 to 25 wt.%). The electrical conductivity has been measured by complex impedance spectroscopy from 303 K to 423 K temperature. The physical parameter and conductivity study indicate to obey the Arrhenius relationship and the frequency dependent conductivity is in consonance with Jonscher's universal power law. The Correlated Barrier Hopping (CBH) model for ion transport is observed to follow in the present glass system. Further investigation of the conductivity has also been carried out to calculate the hopping frequency (ω_p), relaxation time (τ), power-law exponent (n) and decoupling index (R_τ). The enthalpy for migration and free energy have been estimated using the frequency-dependent power-law exponent (n) behaviour. Charge dynamics between local states due to the activated hopping process has been discussed according to Anderson- Drago and Elliot's model. To reinforce the Lithium ion transport study, several physical parameters such as density (ρ), molar volume (V_O), oxygen packing density (OPD), cation concentration (N_{Li}), the mean distance between cations (R'_{LiI}) and the total number of energy states per unit volume at Fermi level $N(E_f)$ have been calculated using various empirical formulae to discuss the present LBP ionic glass system.

1. Introduction

Pure phosphate glass exhibits numerous applications in the working area of fast ion conductors, waveguides, optical switches, fibres and many more [1]. However, pure phosphate glass is hygroscopic in nature and shows deficient chemical durability [1]. Alkali borates have been widely studied because of the significant evolution with composition of both structure and physical properties [2]. Nevertheless, the pure borate glass is normally not useful for any application in the pure form because of the issue with chemical durability and high affinity for water. Therefore, it is used in combination with other oxides which leads to improved chemical durability [3].

Solids containing mobile lithium ions are very significant since they are at the peak of scientific interest in the quest for an efficient energy storage system. There is a requirement for a high degree of disorderliness to have fast ion diffusion in the ionic glass. The fast ion conducting solids containing H^+, Li^+, F^- are usually rich in chemical structural or morphological defects and used for energy storage device application [4]. Alkali oxide glass compositions have been widely studied because of the significant evolution in both structural and physical properties [2,5]. With this background, among all alkali cations, lithium appears to be the most advantageous for electrochemical applications because of its small size, low mass and high electropositivity [2,6–8]. According to Ingram et al; superionic conductors are the compounds (glassy/ crystalline) in which the highest conductivity can be envisaged when the lithium halides added to the parent system [9]. The system containing lithium halides such as *LiI, LiCl, LiBr* showed the highest conductivity and can be treated as superionic compounds [10]. Among all the lithium halide compounds, the *LiI* (hard acid-soft base compound) loosened up Li^+ cations very easily and shows ion transport in a glass system. Takada et al; [11] has also reported that the Lithium iodide based solid electrolytes are known for the highest ambient conductivity. Several research articles on lithium iodide doped solid electrolytes are reported, $Li_3PO_4-Li_2S-SiS_2$ lithium ion conducting sulphide glass has been elucidated by Shiego Kondo and Takada et.al., [11], such as $LiI-Li_2WO_4$ solid electrolyte has been studied by Arofet.al; [12] and $LiI-AgI-B_2O_3$

* Corresponding author.
E-mail addresses: vaishali.adhwaryu@ldce.ac.in (V.A. Adhwaryu), dkkanchan.ssi@gmail.com (D.K. Kanchan).

https://doi.org/10.1016/j.jnoncrysol.2022.121474
Received 9 November 2021; Received in revised form 4 January 2022; Accepted 4 February 2022
Available online 12 February 2022

mixed with V_2O_5 has been analysed by Mogus et.al. [13].

Usually, the network former is the building block of a glassy electrolyte. The addition of metal oxide modifies / alters the parent network and a result, Non-Bridging Oxygen (NBOs) are produced. Furthermore, the dopant is added to acquire mobile ions (cation) for ionic conduction [12]. Alkali ions and/or transition metal ions doped oxide glasses have been extensively investigated for their electrical properties due to easy preparation and wide applications [1,12,14]. The silicate, borate, phosphate, tellurite, boro-vanadate and boro-phosphate glasses have been studied largely by worldwide researchers [1,4,10–20]. With the addition of modifier oxide into the borate and phosphate network, the borate network gets polymerised and changes from trigonal BO_3 to tetrahedral BO_4 while the phosphate network gets depolymerised, and chain like structure turn into the tetra and trigonal units. When the modifier oxides are added to the network, the positive charge of modifier cations compensates the negatively charged non-bridging oxygen sites of the parent framework [15,16]. Several studies of the mixed glass formers (Boro-phosphate) with alkali metal oxide (Li_2O, Na_2O, K_2O) have been reported in the literature so far [10,20].

Lithium and its compounds have several industrial applications, including heat-resistant glass and ceramics, lithium batteries, and lithium-ion batteries. Therefore, there is still a scope to investigate the details related to conduction mechanism study in lithium iodide doped borophosphate glass (LBP) *LiI* doped borophosphate glass can also be termed as *solid electrolyte glass system*. The cause of the change in electrical conductivity (as a function of *LiI* concentration) of the present glass electrolyte is either the mobile charge carrier concentration and/or its mobility. Analysis of electrical conductivity and its Li^+cation transport mechanism using experimental and calculated from empirical relations data is the highlight in the present study. It is significant to understand conductivity using impedance spectroscopy, and subsequently, activation energy for ion conduction, hopping frequency (ω_p), decoupled ion index (R_τ), and the number of energy states at the Fermi level $N(E_f)$ were analysed to understand the theoretical model related to the present glass electrolyte system.

Therefore, it is interesting to study systematic variations of LiI salt in an otherwise very rigid boro-phosphate glassy system. In the present system, we have varied the ionic salt LiI in $x(LiI) : [(100-x).(60Li_2O : 8B_2O_3 : 32P_2O_5)]$ to understand how ionic conduction occurs in a rigid lithium boro-phosphate glass system.

NOVELITY:

- Study of Charge / ion transport mechanism due to LiI in a lithium boro-phosphate glass system
- Temperature and composition dependency on charge transport through the glass matrix.
- Confirmation of Correlated Barrier Hopping (CBH) mechanism by simulating theoretical and experimental parameters in the present glass system.

2. Experimental Procedure

In the present study, composition for the glass samples of $x(LiI) : [(100-x).(60Li_2O : 8B_2O_3 : 32P_2O_5)]$ with x ranging from$x =$ 0 to 25 wt.%, were prepared using melt quench method, wherein analytical grade reagents likeH_3BO_3, $NH_4H_2PO_4$, Li_2O, and LiI chemicals were used [21,22]. The amorphous nature of samples had been examined by X-rays diffraction technique (XRD) in $Cu-K\alpha$ radiation using the Bruker Discovery-8 X-ray machine. The absence of any single sharp peak in the XRD signifies the formation of a homogeneous Lithium borophosphate glass even after an addition of *LiI*.The vibrational modes of various molecular bond and their structural study were carried out by employing Infrared spectroscopy. The Infrared spectrum was recorded using JASCO FTIR-4000 machine in the wavenumber range of 400 – 2000 cm^{-1}at a resolution of 4 cm^{-1} by using the standard *KBr* method. For the *KBr* method, the *IR* grad *KBr* and sample specs in a proportion of 100 : 1 were used for a pellet ($\sim 0.5-1$ *mm* thick) preparation. For electrical conductivity measurement, as a part of electrode preparation, the glass beads were cut and polished in rectangular shape and then coated by the silver paste. Solartron-1260A (frequency response impedance analyser) was used to measure conductivity over a wide frequency range from 1 *Hz* to 32 *MHz* and the temperature range from 303 *K* to 413 *K*.

A complex non-linear least square (CNLLSQ) fitting model was used to analyse impedance spectra using soft tools such as Z-plot, origin8.1 and electrochemical impedance analyser (EIS). The density (ρ) value of glasses, obtained by Archimedes' principle, were used to calculate the various physical parameters such as molar volume (V_m), lithium-ion concentration (N_i), the mean spacing between cations (R'_{LiI}),oxygen packing density (OPD) and oxygen molar volume (V_O).

3. Results and Discussion

3.1. Fourier Transform Infrared Spectroscopy (FTIR) Study

Several absorption bands of the LBP glass system are seen in the recorded IR spectra shown in Fig. 1. The band positions and their assignments are present in Table 1. Absorption bands at the wavenumbers 768 cm^{-1}, 1103 cm^{-1}, 1116 cm^{-1},1240 cm^{-1}, 1283 cm^{-1}, 1334 cm^{-1},1383 cm^{-1}, 1400 cm^{-1} and 1640 cm^{-1} have been observed in the IR spectra to study the present glass system. The absorption band at 768 cm^{-1} corresponding to the $B-O-B$ linkage bending in borate network structure [20,22-27]. The characteristic peak at 1103 cm^{-1} confirms the presence of PO_2 units in the pyro- and metaphosphate group [27,30]. In the lithium borophosphate glass series, $P-O-B$ linkages have signature peak at 1116 cm^{-1} wavenumber [38]. The asymmetric stretching vibration of the $P-O-P$ bond is observed at 1240 cm^{-1} [20,31] while asymmetric stretching vibration of $B-O$ bonds of BO_3 unit shows the characteristic peak at 1283 cm^{-1} [32,33,36]. A characteristic peak near about 1334 cm^{-1} reveals the presence of borate units in pyro- and ortho- borate group [27]. The manifestation of bridging oxygen molecules between triangular borate unit and the tetragonal borate unit is observed at 1383 cm^{-1} [27].The 1384 cm^{-1} is observed probably due to $P=O$ bond and the asymmetric vibration modes of $P-O-P$ link [23,37]. The stretching vibration at 1400 cm^{-1} is associated with the $B-O$ bond with the non-bridging oxygen atoms in penta-, ortho-, pyro- borate groups [27,29,38]. The peak appears at 1640 cm^{-1} attributed to the asymmetric stretching mode of relaxation

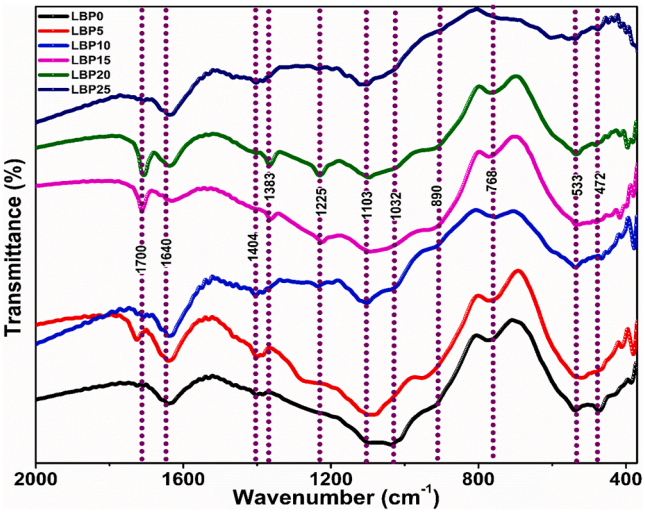

Fig. 1. FTIR absorption spectra of all glass samples between 400 cm-1 to 2000 cm-1 wave number.

Table 1
Band positions and assignments of IR bands of present glass system.

Wavenumber (Cm^{-1})	Mode Of Vibration	Assignment Of IR Band	Reference
~ 755-770	Symmetric stretching (ν_s)	P – O – P in rings of the bridging oxygen atoms Transformation of borate units from BO3 to BO4 B – O – B linkages bending in borate network	[12,22,23, 25-30]
~1100-1150	Asymmetric stretching (ν_{as}) Symmetric stretching (ν_s)	P – O – P of polymeta chain of (PO^{3-}) unit Non-bridging oxygen from terminal P – O bond and PO_3unit B-O stretching of BO4 units in various borate rings (di-, tri-, tetra-, penta borate groups)	[27,31,32, 33,34]
~1225-1240	Asymmetric stretching (ν_{as})	B – O stretching vibrations ofBO^{3-} units in penta-, ortho-, pyro- and metaborate groups Metaphosphate $(PO_2)^-$ group P = O in PO_4structural unit with one Non-bridging oxygen and change in $P-O-$ *P*linkage due to formation of $P-O-B$ link	[20,25,31, 32,35,36]
1283	Asymmetric stretching (ν_{as})	$B-O$ bonds of BO_3 unit	[32,33,36]
~1334 -1383	Symmetric stretching (ν_s)	Borate unit in pyro- and ortho-borate group. Bridging oxygen between BO_3 and BO_4 group P = O in NBO atom of phosphate chain $PO_2$of non-bridging oxygen in a phosphate chain	[12,23, 27, 30,36,37]
~1400-1404	Asymmetric stretching (ν_{as}) Anti-symmetric stretching	Borate triangle unit (BO^-). B – O bonds associated with NBO in penta, ortho, pyro borate group	[27, 29, 32, 36, 38]
1627	Asymmetric stretching (ν_{as})	B – O bond present in trigonalBO_3units	[36]

vibration in B-O bond present in trigonal BO_3 units [36].

Upon *LiI* addition in the lithium oxide modified boro-phosphate glass, the continuous breakdown of the borate ring type structure resulting into polymerisation of borate network can be envisaged as the wavenumber shifting from 768 cm^{-1} to 780 cm^{-1} for LBP25 sample, corresponding to $B-O$ stretching of BO_4 units. Similar observations have been reported by H. Tunt et al; [26] and N.J. Kim [20] and T. Q. Leo et al; [27] have reported that the conversion from BO_3 to BO_4 unit ultimately polymerises the borate network in the glass structure. From pure LBP sample to LBP25 sample the band at 1103 cm^{-1} goes broadened signifies the formation of tetragonal borate unit. The absorption band at 1116 cm^{-1} shows shift to ~ 1096 cm^{-1} possibly due to weakening of the double bond character in PO_4 polyhedra, which concurs with reported research work by Kabi and Ghosh [38]. With the addition of LiI, the band at 1240 cm^{-1} appears in LBP10 sample broadens gradually till LBP25 and is ascribed the changes in $P-O-P$ linkage due to formation of cross linking through $P-O-B$ bond formation. The blur peak at 1383 cm^{-1} is seen in pure LBP glass, which is shifting to the lower wavenumber 1357 cm^{-1} for LBP25 sample, which confirms the elongation of BO_3 units and eventually converting to tetragonal borate group as BO_4 [27,36]. The peak at 1400 cm^{-1} wavenumber is assigned to the non-bridging oxygen bonded with $B-O$ link and remains unchanged even with addition of *LiI*. The wave number 1640 cm^{-1} observed for LBP0 sample gradually shifts towards 1627 cm^{-1} for LBP25, suggests disappearance of the trigonal BO_3 units. It is interesting to note that the peak at 1640 cm^{-1} [36] wave number shifts to lower wave number side i.e., at 1627 cm^{-1} with the addition of *LiI*, indicating the gradual structural changes in the trigonal borate units.

With the gradual increase in *LiI* concentration, the frequency of most of the units of glass formers shifts to the lower wave number side attributing the expansion of the glass structure due to the polymerization of borate and phosphate network. A transformation from BO_3 to BO_4 units due to polymerisation of borate network and depolymerisation of phosphate network from PO_5 units to PO_4 units in the structure is expected.

3.2. Physical Properties

The physical parameters of the present glasses are given in Table 2. It is observed that the density (ρ) increases from *2.46 g/cc* to *2.50 g/cc* with the addition of *LiI* salt content from 0 to 25 wt.%. This could be due to increase in molecular weight of iodide ion (Molecular Weight. *126.9045*) in *LiI*. The molar volume (V_m) increases from 41.2346 cc/mole to 43.8829 cc/mole with Lithium salt concentration confirming the expansion of the glass structure. It is also observed that the structure is accompanied by a decreasing oxygen packing density (OPD) from *59.1736 (mol/l)* to *42.2038 (mol/l)*while oxygen molar volume (V_O) increases from 16.90 to 23.70 means volume expansion of the glass with the addition of *LiI*. The glass transition temperature (T_g) is directly related to the composition of glasses. In the present system, the glass transition temperature decreases (not significantly) from 1063.5 *K* to 1061.1 *K* with *LiI* addition. It is clearly observed from FTIR that the more number of tetragonal borate unit (BO_4) units are formed with Lithium salt addition.

3.3. Conductivity Analysis

The impedance spectra shown in Fig. 2(a-f) of the LBP glass series exhibit a semi-circle at the high frequency corresponding to the bulk conduction and the inclined spike observed at the low frequency region due to electrode polarization phenomena. As we increase the salt concentration in the glass, second semicircle starts building up and the bulk resistance of the semicircle at high frequency decreases. At high temperature, the thermally stimulated cations contribute to ionic conductivity [13]. The semicircle arc corresponds to the bulk conduction whereas the spur is due to the electrode polarization in Fig. 2(a-f). The presence of the spur at higher amount of *LiI* points to the blocking of *Li* ions at the electrodes. It should be noted that the spur appears in the high temperature region suggesting the thermally stimulated mobility of ions. Fig. 3 shows the Nyquist plot and fitted equivalent circuit for the LBP25 glass at 373 *K* temperature. DC Conductivity is calculated using the following equation.

$$\sigma_b = \frac{t}{R_b A} \quad (1)$$

The enhancement of conductivity may be due to the increasing ionic contribution with the concentration of *LiI* [13]. Fig. 4 illustrates the dc conductivity as a function of the inverse temperature for all the samples. The activation energy required for the conduction process is obtained using the slope of the DC conductivity plot given in Fig. 4, the linear fit has the goodness of fitting ranging from 0.97532 -0.99819. The dc conductivity and activation energy plot is shown for different salt concentrations in Fig. 5. The activation energy (E_σ) required for the conduction process is calculated using the Arrhenius relation. With the addition of *LiI*, as given in Table 2, the value of activation energy seems to decrease. The decrease in activation energy means decrease in the electrostatic binding energy as well as the strain energy needed for the easy passage to the lithium and silver ions. The slight change in glass transition temperature (T_g) is observed which may be due presence of rigid framework borate structure. The continuous decrement in the jump

Table 2
Various physical parameters of the LiI-Li_2O-B_2O_3:P_2O_5 glasses.

Physical parameter (with uncertainty using standard deviation)	LBP0	LBP5	LBP10	LBP15	LBP20	LBP25
LiI concentration (x in wt.%)	0	5	10	15	20	25
Density: (gm/cc) with uncertainty ± 0.02	2.46	2.46	2.47	2.48	2.48	2.50
Molar Volume: V_m (cc/mole) with uncertainty ± 0.4	41.23	41.89	42.36	42.90	43.50	43.88
Oxygen Packing density:OPD (mol/l)with uncertainty ± 0.3	59.17	55.34	51.84	48.34	44.88	42.20
Oxygen Molar volume: V_O (cc/mol) with uncertainty ± 0.1	16.90	18.07	19.29	20.69	22.28	23.69
Glass transition temperature: T_g (K)	1063.5	1063.1	1062.9	1062.7	1061.6	1061.1
No. of cations from Li_2O: N_1 (x 10^{21}/cc)with uncertainty ± 0.05	8.76	8.20	7.68	7.16	6.65	6.25
No. of cations from LiI: N_2 (x 10^{21}/cc)with uncertainty ± 0.005	-	0.72	1.42	2.11	2.77	3.43
Total number of cation: N_i (x 10^{21}/cc)with uncertainty ± 0.09	8.76	8.92	9.10	9.27	9.42	9.68
U_M at 373K: ± 0.01 (eV)	7.42	4.95	3.165	3.065	2.30	2.03
R_{min} (1MHz) at 373K (Å) with uncertainty ± 0.6	59.22	79.11	1.27	98.05	1.46	1.52
Mean distance between cations: R'_{LiI} (Å)with uncertainty ± 0.03	-	11.16	8.89	7.80	7.12	6.63
$N(E_f)$ x10^{20} $(eV)^{-1}$/cc with uncertainty ± 0.02	-	1.60	3.20	4.78	7.31	9.24
Activation energy for conduction: E_a (eV)with uncertainty ± 0.008	1.12	1.08	1.06	1.05	0.91	0.89
Hopping freq. at 373 K: ω_p (x10^6 Hz) with uncertainty ± 0.01	0.14	0.49	0.58	1.18	1.32	2.25
Total Enthalpy: $H=H_m + H_f$(eV) with uncertainty ± 0.008	1.20	1.11	1.09	1.08	0.95	0.92
Enthalpy of migration: H_m (eV) with uncertainty ± 0.008	0.88	1.05	1.05	1.06	0.93	0.90
Enthalpy of free energy: H_f (eV) with uncertainty ± 0.002	0.32	0.06	0.04	0.03	0.02	0.02

distance of Li ions, and increase in the molar volume (V_m) values also confirm and acknowledge the variation of activation energy and conductivity.

The conductivity enhancement at various temperature/ salt concentration is related to the number of charge carriers and/or the mobility of the thermally stimulated charge carriers. Tetrahedral sites are formed by the network former *(B_2O_3-P_2O_5)*, into which the added salt enters at interstitial positions and induces the formation of non-bridging oxygen (NBO). And the resulting NBO converts the triangular borate units into a tetrahedral borate unit. The decrease in activation energy and increase in conductivity with increasing *LiI* content is probably causes a weaker degree of cross-linking the glass network. This, in turn, leads to a decrease in the electrostatic binding energy.

The ratio of $\tau_s(T_g)/\tau_m(T_g)$ measures the decoupling index$R_\tau(T_g)$ of the ions in the host matrix, where $\tau_s(T_g)$ and $\tau_m(T_g)$ arethe average structural and the conductivity relaxation times at the glass transition temperature T_g respectively. It is to be noted that $R_\tau(T_g)$, which describes the extent to which the motion of the conducting ions in the glassy matrix, can be decoupled from the viscous motion of the glassy matrix at T_g[39].According to Fig. 6, in the present system, the decoupling index, R_τ increases with the increase of *LiI* content as well as with temperature. It means, motion of the conducting *Li* ions in the glassy matrix is getting decoupled from the viscous motion of the glassy matrix at T_g with composition as well as with temperature, hence continuous rise in conductivity can be expected.

3.4. Frequency dependent conductivity

The ac conductivity of glass samples with all compositions have been recorded and calculated for the temperature range 303 *K*-413 *K* and frequency range 1 Hz-32 MHz. It is evident from Fig. 7(a) and 7(b) that the ac conductivity shows its dependency not only on temperature but also on composition. For the studied frequency range, it is observed that with *LiI* content, frequency dependent conductivity $\sigma'(\omega)$ shows a constant behaviour at frequency and then starts increasing depicting its relaxation region. Meenakshi Dult et.al., in boro-silicate and Mahmoud et.al., in lithium-bismuth borate glasses observed the similar observations [40,41]. Frequency dependent conductivity at an arbitrary temperature value is shown in Fig. 7(a). Two significant regions namely plateau and dispersion are present in the frequency dependent conductivity $(\sigma'(\omega))$ in shown Fig. 7(a & b).At low frequencies the plateau region is observed, where the random distribution of the charge carriers by activated hopping results in frequency-independent conductivity. In the plateau region, the frequency range width increases with temperature. When the curve is seen flat in the low frequency region, its corresponding conductivity value can be approximated as the dc conductivity (σ_{dc}), whereas, the dispersion region is observed at high frequency. The conductivity $\sigma'(\omega)$ goes on increasing with an increase in frequency (ω), which shows high dependence on frequency. The conductivity spectra become more dispersive with the increase in frequency and seems to merge in high frequency region. When the temperature rises, the width of the dispersive region decreases. The samples from LBP15 starts showing another dip at lower frequency region attributing

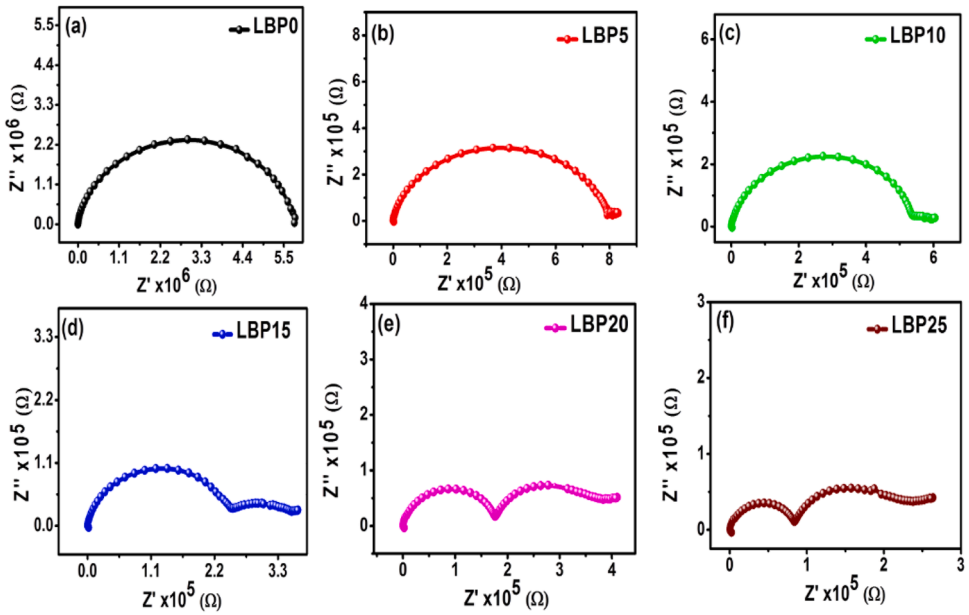

Fig. 2. (a-f) Nyquist plot of all glassy electrolytes with xLiI in the LBP glass system (x=0-25 wt.%) at 373 K temperature.

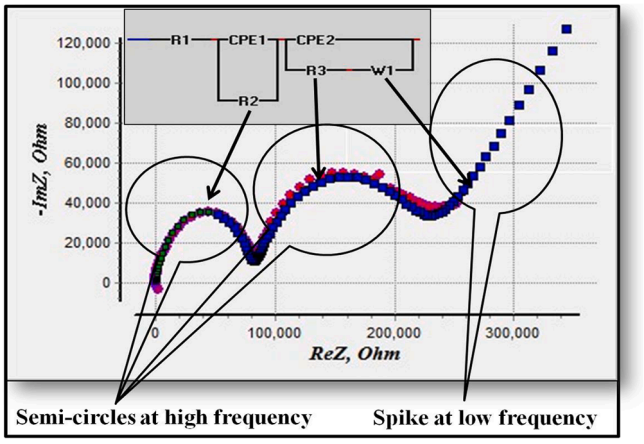

Fig. 3. Nyquist plot fitting and its equivalent circuit for LBP25 sample at 373 K. (solid line is just a guide for eyes).

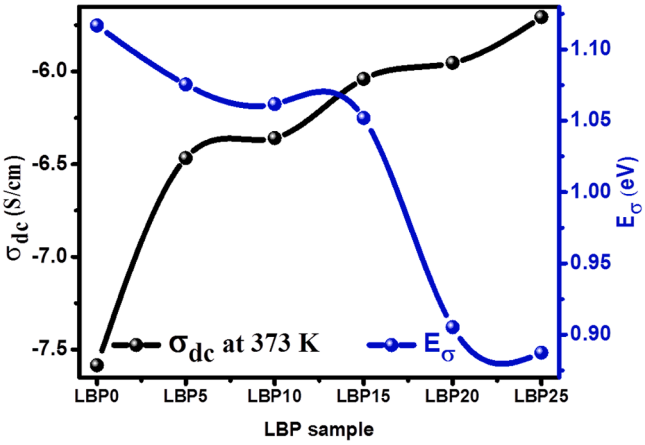

Fig. 5. Variation of σ(dc) with activation energy E(σ) for all glass compositions.

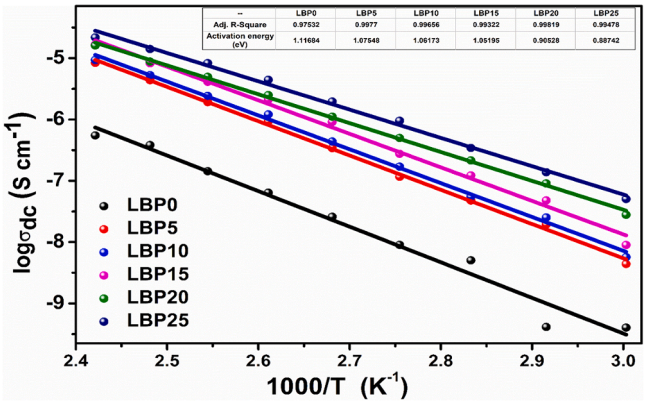

Fig. 4. Log of dc conductivity vs. 1000/T plot of all glass samples. (Sphere indicate the data point and the straight line reflects linear fitting of the trend- a guide to the eyes).

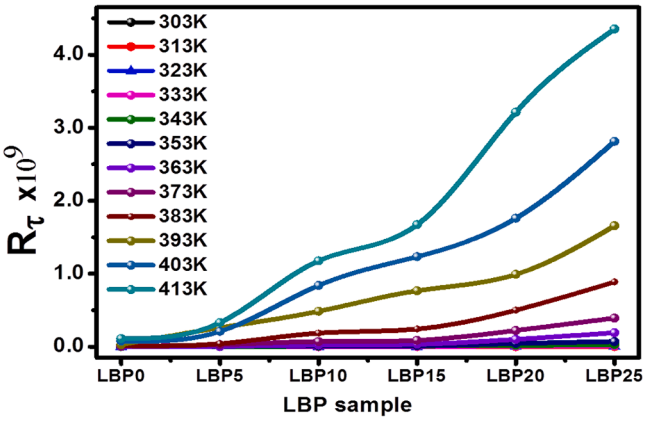

Fig. 6. Decoupling index (R_τ) at various temperatures for all glass compositions.

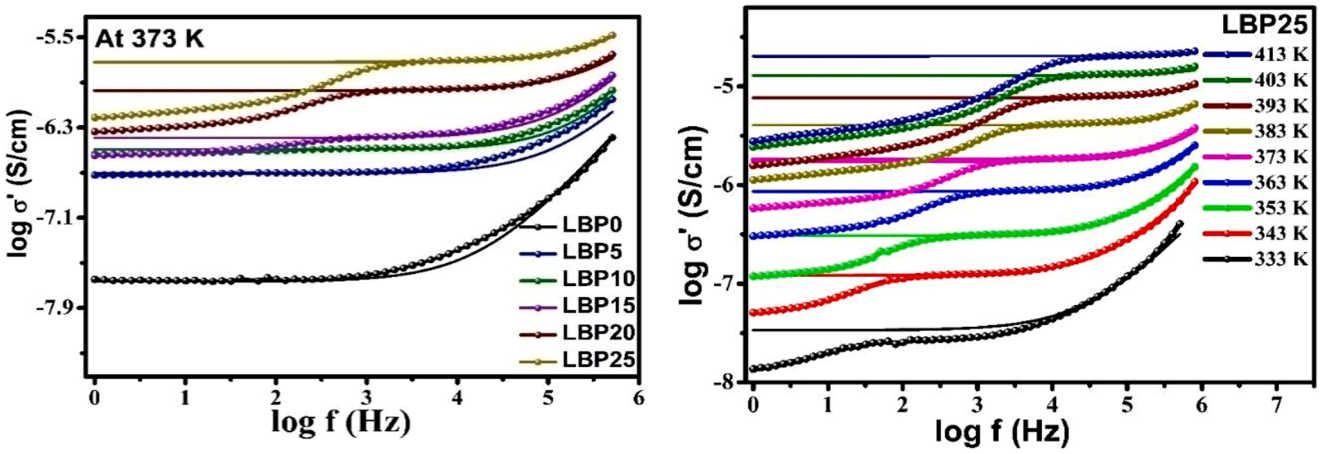

Fig. 7. **(a)** Variation of ac conductivity as a function of log frequency of all glass samples with at 373 K. (Solid straight line shows the JPL fitting). **(b)** Variation of log ac conductivity of LBP25 as a function of log frequency at different temperatures. (Solid straight line shows the JPL fitting).

to building up of polarisation. The changeover of conductivity shifts to the higher frequency as the temperature increases, because the mobile ions acquire thermal energy and hence cross the barrier potential more easily. In general, the frequency dependent ac conductivity is given by Jonscher's power law [22].

$$\sigma_{ac} = \sigma_{dc} + A(\omega)^n \tag{2}$$

where A is the characteristic parameter, ω is the radial frequency $(\omega = 2\pi f)$ and n is the power exponent which depends on the temperature(commonly known as $n(T)$) and the frequency. The fitting of the experimentally measured data of frequency dependent conductivity σ_{ac} at different temperatures, gets the values of σ_{dc}, A and n.

Fig. 7(a) shows the plot of ac conductivity fitted with Jonscher's universal power law for all the glass samples at 373K and Fig. 7(b) depicts the frequency response of ac conductivity for the glass composition LBP25 at different temperatures. The increase in the thermally activated cations (total number) and/or their drift velocity is observed with rising in the temperature is responsible for the observed rise in conductivity in the present glass samples. M. Gabr et al., P. V. Rao et al; and other research groups have also reported the similar observations in different glass systems [41–44]. In the present glass system, from LBP0 to LBP25 sample, the total number of cations $N_i(Li^+)$ (due to Li_2O and /or LiI) is raised from $8.764x10^{21}/cc$ to $9.682x10^{21}/cc$as mentioned in Table 2. The room temperature conductivity ranges from 10^{-8} to10^{-6} S/cm for LBP0 to LBP25 samples respectively. The straight line variation of dc conductivity $(\sigma_{dc})$with the inverse of temperature $(1/T)$ confirms the Arrhenius relation (Eq. 3).

$$\sigma_{dc}(T) = \sigma_0 e\left(\frac{-E_a}{kT}\right) \tag{3}$$

Here σ_0 is the material dependent pre-exponent factor, E_a is the activation energy for conduction, k is the Boltzmann constant, and T is the temperature (in Kelvin).Fig. 4 shows the variation of $log\ (\sigma_{dc})$ versus $1000/T$ for the present glass series. From its linear fit, activation energy (E_a) has beencalculated andis shown in Table 2 for all the samples. The activation energy for the conduction process decreases with the increase in LiI concentration. This activation energy corresponds to the trap level located below the conduction band [40].The following relations Eq. 4 & (5) are applied to calculate the density of states $N(E_f)$ of thermally activated electron hopping at the Fermi level (E_f) and mean distance between two cations (R') [13,40].

$$N(E_f) = \frac{3}{4\pi R'^3 E_a} \tag{4}$$

$$R' = \sqrt[3]{(1/N)} \tag{5}$$

where $N(E_f)$ is the density of energy states at Fermi level, R' is the mean distance between two Li-cations, N_i is the concentration of cations and $E_a$is the activation energy. From Table 2, the glass network of LBP5 to LBP25 sample, the value of $N(E_f)$ reasonably increases from 1.60×10^{20} eV^{-1} cm^{-3} to 9.24×10^{20} $eV^{-1}cm^{-3}$ which is indicative of the augmentation of defect energy states or free charge carriers. The mean distance between lithium cations (R'_{LiI}) gradually decreases (Table 2), which manifests the ease of movement for ion transportation.

In order to understand the interaction between the ion and the network, frequency power exponent *(n),* has been included into discussion. The smaller value of $n(T)$ signifies the higher degree of modification in the network [22,40,42]. In the present system, analysis of the power exponent $n(T)$confirms the hopping mechanism involved in conductivity. When an AC field is applied to the system, the value of $n(T)$ is used to determine the mechanism of conduction [45]. In the studied temperature region, a decrease in $n(T)$ value is observed, which is assumed to be associated with the Correlated Barrier Hopping mechanism for conduction [40,42]. The $n(T)$ behaviour of all the samples at different temperatures is depicted in Fig. 8, where the error bar reflects the error analysis using the standard deviation source method. The mobile ion concentration factor K' is an important factor in conductivity. Furthermore, looking into the total charge carrier concentration(K')

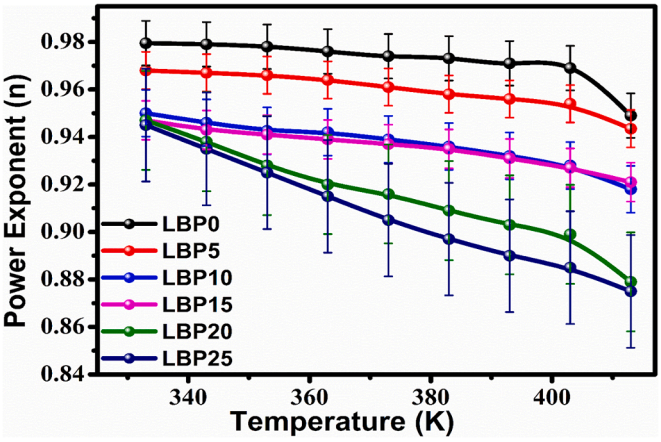

Fig. 8. Frequency exponent (n) as a function of temperature for all the glass compositions. (Standard deviation is used as the error source which is represented by error bar).

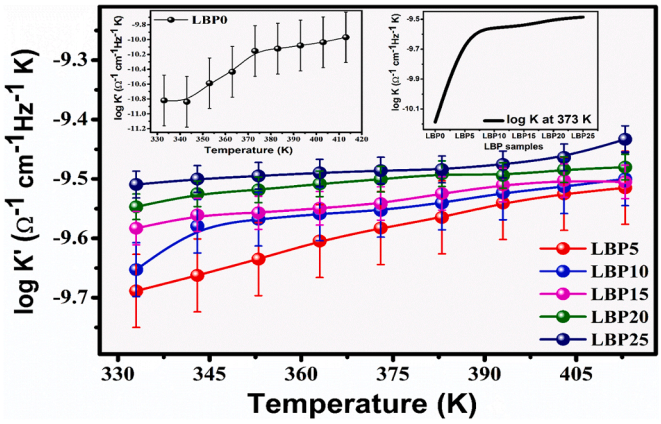

Fig. 9. Mobile ion concentration K' as function of temperature for LBP glass compositions. (Deviation in carrier concentration is given in form of error bar) Insets: (I) trend of log K' for LBP series at 373 K, (II) For LBP0, variation of carrier concentration with temperature.

(Fig. 9), the rising trend of the charge carrier concentration (K') from LBP5 to LBP25 sample is consistent with the conductivity behaviour. With respect to temperature the deviation in K' value for each glass sample is shown in Fig. 9 using error bar. K' is dependent on the values hopping frequency, temperature and dc conductivity. A fraction of the total number of charge carriers (n') is mobile when the conduction process occurs via a defect mechanism, which is given by mathematical expression,

$$n' = Ne^{\left(\frac{-G_f}{kT}\right)} = Ne^{\left(\frac{S_f}{k}\right)}.Ne^{\left(\frac{-H_f}{kT}\right)} \quad (6)$$

The parameters associated with the dissociation of cations from their original sites next to the charge compensation centre are N, the total charge carriers, entropy (S_f), enthalpy (H_f), and free energy (G_f), as mentioned in Eq. (6). The cross over (hopping) frequency (ω_p) given by Eq. (7) and the DC conductivity, in the form of dissociation process, is given by Eq. (8)

$$\omega_p = \omega_0 e^{\left(\frac{S_m}{k}\right)}.e^{\left(\frac{-H_m}{kT}\right)} \quad (7)$$

$$\sigma_{dc} = \frac{NZ^2e^2d^2\gamma\omega_0}{kT} e^{\left(\frac{S_f+S_m}{k}\right)} e^{\left(-\frac{H_f+H_m}{kT}\right)} \quad (8)$$

Here, an attempt frequency is called ω_0, the parameters related to migration are entropy (S_m) along with enthalpy (H_m), the geometric and correlation constant shown as γ, while jump distance appears as d. According to Jain and Mundy [46], the explanation of the conduction mechanism in ionic glasses can be through the conductivity versus an inverse of the temperature plot. The total enthalpy incorporates mainly two components such as free energy (H_f) and migration (H_m), which elucidate the dissociation of the cations from their original site next to the charge compensating centre [40]. In the present system, the value estimated using the linear fitting (with the goodness of fit range 0.9854-0.9990) of the logarithmic function of hopping frequency versus the inverse of a temperature graph shown in Fig. 10(a). Using Eq. (7) and (8), the log ω_p and log $(\sigma_{dc}T)$ versus $1/T$ are plotted and shown in Fig. 10(a & b).The value of log $(\sigma_{dc}T)$ is fitted linearly (Fig. 10(b)) with the value of Adj. R-square ranging from 0.98564-0.99888 in order to obtain the value of enthalpy with respect to the reciprocal of temperature. The values of ω_p are shown for the temperature 373 K in According to Table 2, the values of ω_p, for the temperature 373 K, increase from 0.13809 MHz to 2.24675 MHz with the lithium salt addition. The values of total enthalpy H_f+H_m and the enthalpy for migration (H_m) are estimated using slops of linearly fitted plots (Table 2). The data presented in Table 2 shows the calculated values of H, H_f and H_m for all the glass samples. For the current system, the value of H_f is higher than zero as given in Table 2. It means that the total number of charge carriers exceeds the total number of mobile charge carriers at a given instance. It is clear that with *LiI* content, the conductivity of the present glass system increases not only due to the mobility of charge carriers but also due to their concentration [40].

3.5. Ion transport Model

Under AC field, the variation of $n(T)$ with temperature varies differently under different conduction mechanism models. In the overlapping-large polaron tunnelling (OLPT) conduction mechanism [47], the exponent $n(T)$ decreases with increasing temperature to a minimum value at a certain temperature and then begins to increase with increasing temperature. In the quantum mechanical tunnelling (QMT) [48]conduction mechanism, the exponent $n(T)$ is almost equal to 0.8 and increases slightly with increasing temperature or is independent of temperature. In the non-overlapping small polaron tunnelling (NSPT) conduction mechanism, the exponent $n(T)$ increases with increasing temperature [49]. While, the value of $n(T)$ decreases with the increase in temperature in the correlated barrier hopping (CBH) conduction mechanism [40,50–54]. According to CBH model, the n(T) can be expressed as Eq. (9).

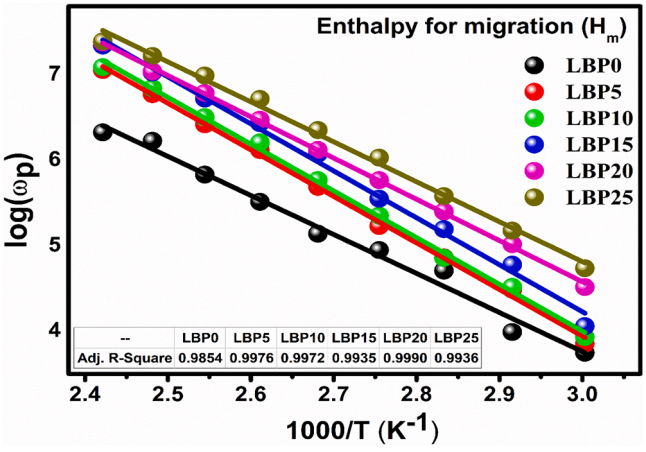

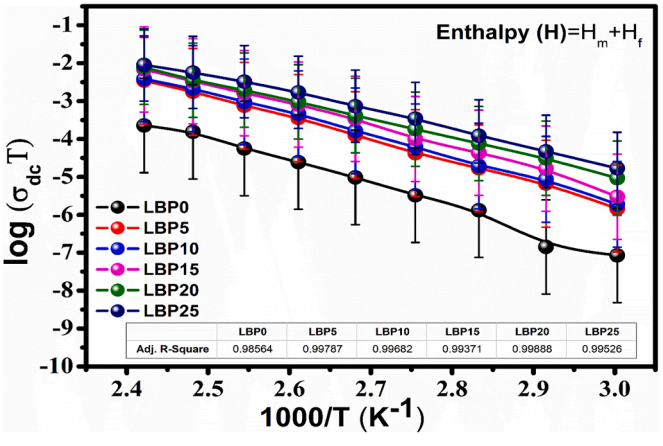

Fig. 10. **(a)** Enthalpy for migration (H_f) estimated using hopping frequency log(ω_p) vs. inverse of temperature(1/T) graph. (Goodness of linear fitting is shown in the table given as Adj. R-Square and the straight line is the guide for the eyes). **(b)** Total enthalpy (H) derived from the slope of linear fitted log (σ_{dc} T) vs. inverse of temperature (1/T) plot. (Goodness of linear fitting is shown in the table given as Adj. R-Square and the straight line is the guide for the eyes).

$$n(T) = 1 - \frac{6kT}{U_M + kT\ \ln(\omega\tau_0)} \tag{9}$$

If the maximum barrier height at a given temperature is given as $U_M \gg kT$, $\omega\tau_0 \sim 1$, where τ_0 is the time constant for downward jump. Now, the modified values of the frequency dependent power exponent $n(T)$ and frequency dependent hopping distance (R_{min}in Å), when the field is applied, can be given as;

$$n(T) = 1 - \frac{6kT}{U_M} \tag{10}$$

The calculated values of maximum barrier height (U_M), effective barrier height (U_H), and frequency-dependent hopping distance (R_{min}) are also given in Table 2.

$$R_{min} = \frac{e^2}{\pi\varepsilon' \varepsilon_0 U_M} \tag{11}$$

Here the overlapping of the Coulomb well of the neighbouring sites separated by R (Li-Li distance), results in the lowering of the effective barrier height from U_m to a value U_H, when a charge carrier hops between site pairs over the potential barrier separating them, it is given by

$$U_H = U_M - \frac{e^2}{4\pi\varepsilon' \varepsilon_0 R} \tag{12}$$

where, e - charge of the carrier, ε'- dielectric constant of a material, ε_0- free space permittivity, R–finite separation between two neighbouring hopping sites *(Å)* and τ_0 is characteristic relaxation time, its typical value $\tau_0\ (= 10^{-13} sec)$ is of the order of vibrational period of an atom.

For neighbouring sites at a separation R, the coulomb wells overlap, resulting in lowering of the effective barrier height from U_M to a value U_H which is given by Eq. 12, where U_M is the energy required to remove the electron completely from the site with $n = 1$ for single-electron hopping and $n = 2$ for two-electron CBH model.

As per CBH model, ac conductivity is given by

$$\sigma_{ac} = \frac{\pi^3}{12} N^2 \varepsilon' \varepsilon_0 \omega R_\omega^6 \tag{13}$$

where N is the concentration of a pair of sites, and $R_\omega$is the hopping distanceat a particular frequency (ω) can be given by Eq. 14

$$R_\omega = \frac{2e^2}{\pi\varepsilon' \varepsilon_0 \{U_M + kT\ \ln(\omega\tau_0)\}} \tag{14}$$

Fig. 11 depicts the value of $n(T)$ as predicted theoretically (line) and as measured empirically (sphere), both decreasing with temperature, with the difference from the measured value displayed by the error bar.

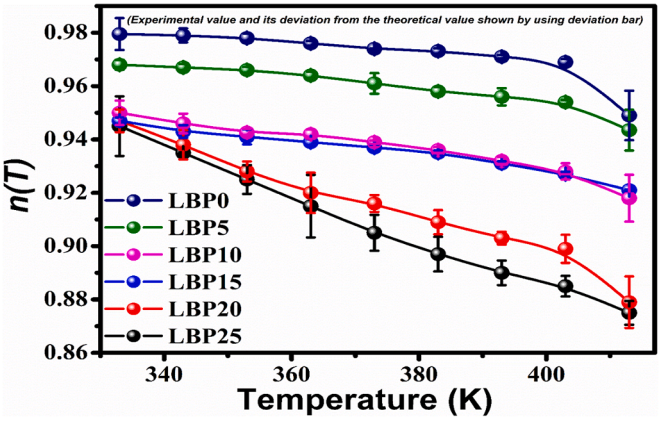

Fig. 11. Comparison of Power exponent (n) value using theoritical equation and experimental data.(The error bar symbolizes the deviation from the experimentally obtain data).

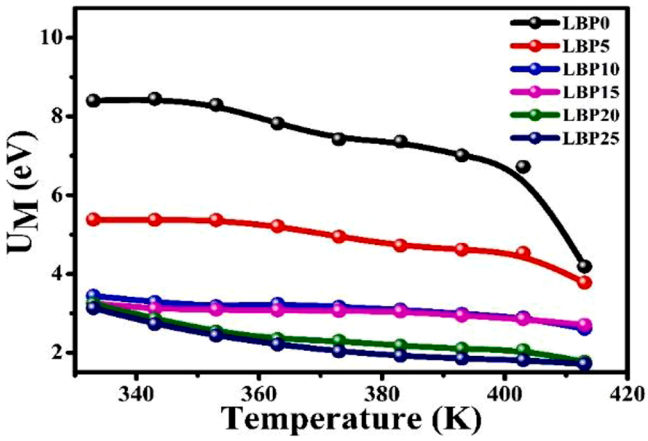

Fig. 12. At various temperature the effective barrier height (U_M) for LBP glass compositions.

Also, It is clear from Fig. 12, that due to an increase in temperature and *LiI* amount in lithium boro-phosphate glass skeleton, the value of barrier height (U_M) decreases, whereas R_{min} decreases with temperature at different frequencies shown in Fig. 13(a) to (d). R_{min} also shows the decreasing trend with temperature (Eq. 11) for all glass compositions shown in Fig. 13(e) which is suggestive of CBH mechanism. Hence, it can be ascribed that all the glass samples follow the CBH model of conduction mechanism for ion transport.

4. Conclusion

The addition of Lithium iodide in $(60Li_2O : 8B_2O_3 : 32P_2O_5)$ glass system has been characterised through various physical, structural and conductivity study. It is interesting to note that the addition of LiI in the glass structure makes it an ionic conductor as the Li ion dissociated from LiI hops and conducts in the glass structure as per CBH model. The glass structure opens more with the addition of LiI content. No major structural modifications of the network and almost no change in glass transition temperature are visible due to the addition of LiI. Depolymerisation of the phosphate chain network and polymerisation of borate network i.e., transformation from ring type structures of BO_3 units of borate chains to BO_4 units in the glass, facilitate the transport of Li ions due to the opening up of the glass network. The glass samples follow the Jonscher's power law for frequency dependent conductivity. The variation of *n(T)* obtained experimentally and the values of *n(T)* calculated theoretically by using R_{min} and U_M values follow the same trend and suggests that in the present glass system, Li^+ ion transport occurs according to Correlated Barrier Hopping (CBH) mechanism.

Confirmation of Authorship- A Cover letter

We, Vaishali Adhwaryu and Prof. D K Kanchan submit this *(REVISED VERSION according to the comments/ suggestions by reviewers and editors)* manuscript entitled '**Effect of Lithium Iodide on transport phenomenon in Lithium Borophosphate glass Electrolyte'** for publication to the Journal of Non-Crystalline Solids.

This manuscript deals with FTIR, TG-DTA, Electro-chemical impedance spectroscopy and discussed the ion dynamics of Li^+ ion in the borophosphate glass electrolyte system in detail. We declare that this paper has not been submitted to any journal/book or conference for publication.

The work has been undertaken without any Government or Non-government funding support. The authors declare that they have no known competing financial interests or personal relationships that could have appeared to influence the work reported in this paper.

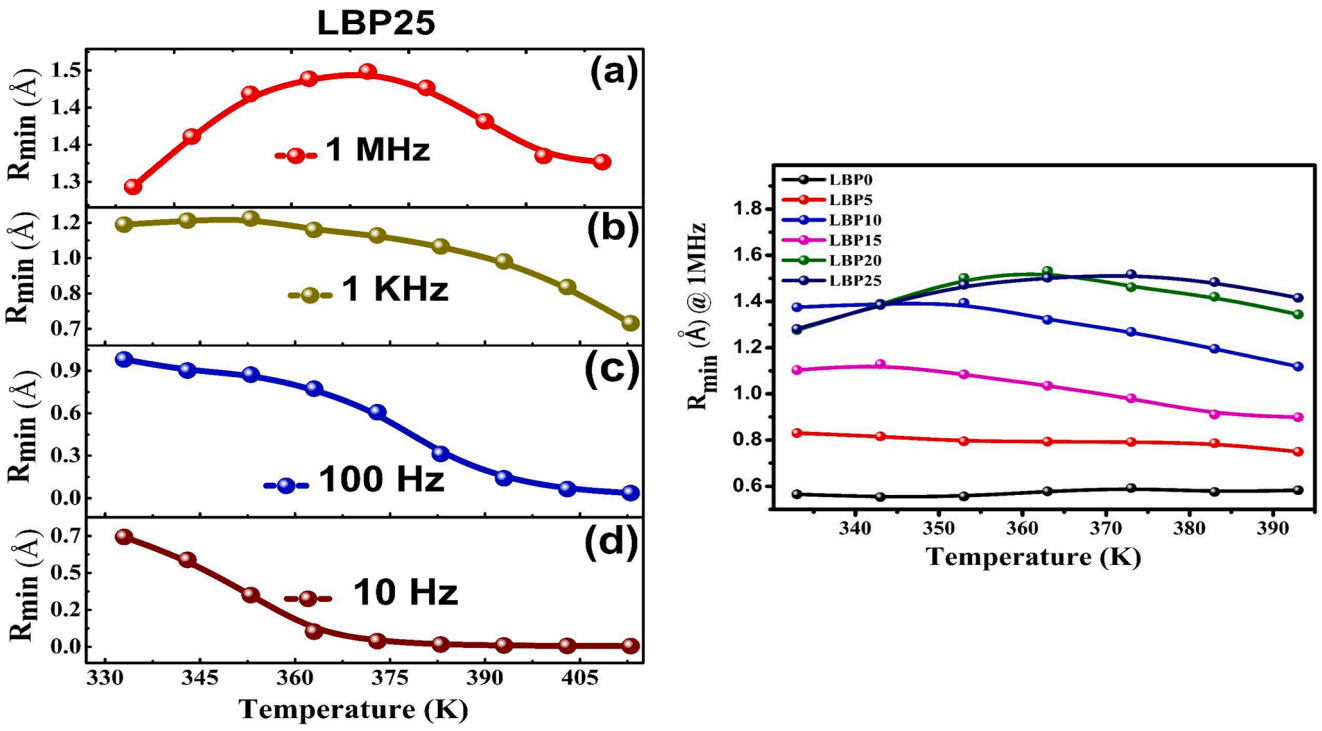

Fig. 13. (a-d) The minimum hopping distance Rmin (ω) at various frequencies for LBP25 sample. **(e).** At 1MHz frequency the minimum hopping distance (Rmin) for all glass compositions at various temperatures.

Data Availability Statement

The necessary data may be made available upon request.

Declaration of Competing Interest

The authors declare that they have no known competing financial interests or personal relationships that could have appeared to influence the work reported in this paper.

Supplementary materials

Supplementary material associated with this article can be found, in the online version, at doi:10.1016/j.jnoncrysol.2022.121474.

References

[1] L Koudelka, et al., in: 2009 IOP Conf. Ser.: Mater. Sci. Eng., 2015, https://doi.org/10.1088/1757-899X/2/1/012015.
[2] V. Montouillout, H. Fan, L. del Campo, S. Ory, A. Rakhmatullin, F. Fayon, M. Malki, Ionic conductivity of lithium borate glasses and local structure probed by high resolution solid-sate NMR, Journal of Non-Crystalline Solids 484 (2018) 57–64, https://doi.org/10.1016/j.jnoncrysol.2018.01.020.
[3] M. Bengisu, Borate glasses for scientific and industrial applications: a review, J Mater Sci 51 (2016) 2199–2242, https://doi.org/10.1007/s10853-015-9537-4.
[4] C.Vinod Chandran, P. Heitjans, Chapter One - Solid-State NMR Studies of Lithium Ion Dynamics Across Materials Classes, Editor(s): Graham A. Webb, Annual Reports on NMR Spectroscopy, 89, Academic Press, 2016, https://doi.org/10.1016/bs.arnmr.2016.03.001. ISSN 0066-4103, ISBN 9780128047125.
[5] A.C. Wright, My Borate Life: An Enigmatic Journey, Int J Appl Glass Sci 6 (2015) 45–63, https://doi.org/10.1111/ijag.12113.
[6] A. Levasseur, M. Menetrier, Borate based lithium conducting glasses, Materials Chemistry and Physics 23 (1–2) (1989) 1–12, https://doi.org/10.1016/0254-0584(89)90013-8. ISSN 0254-0584.
[7] D.D. Ramteke, R.S. Gedam, Study of Li2O–B2O3–Dy2O3 glasses by impedance spectroscopy, Solid State Ionics 258 (2014) 82–87, https://doi.org/10.1016/j.ssi.2014.02.006. ISSN 0167-2738.
[8] D.D. Ramteke, H.C. Swart, R.S. Gedam, Electrochemical response of Nd3+ ions containing lithium borate glasses, Journal of Rare Earths 35 (5) (2017) 480–484, https://doi.org/10.1016/S1002-0721(17)60937-2. ISSN 1002-0721.
[9] Malcolm D. Ingram, A.H. Jean Robertson, Ion transport in glassy electrolytes, Solid State Ionics 94 (1–4) (1997) 49–54, https://doi.org/10.1016/S0167-2738(96)00610-8. ISSN 0167-2738.
[10] Michel Duclot, Jean-Louis Souquet, Glassy materials for lithium batteries: electrochemical properties and devices performances, Journal of Power Sources 97–98 (2001) 610–615, https://doi.org/10.1016/S0378-7753(01)00641-3.
[11] Kazunori Takada, Noboru Aotani, Shigeo Kondo, Electrochemical behaviors of Li+ ion conductor, Li3PO4-Li2S-SiS2, Journal of Power Sources 43 (1–3) (1993) 135–141, https://doi.org/10.1016/0378-7753(93)80110-B. ISSN 0378-7753.
[12] A.H. Ahmad, A.K. Arof, Structural studies and ionic conductivity of lithium iodide-lithium tungstate solid electrolytes, Ionics 8 (2002) 433–438, https://doi.org/10.1007/BF02376058.
[13] A. Moguš-Milanković, L. Pavić, K. Srilatha, Ch.Srinivasa Rao, T. Srikumar, Y. Gandhi, N. Veeraiah, Electrical, dielectric and spectroscopic studies on MnO doped LiI–AgI–B2O3 glasses, J. Appl. Phys. 111 (2012), 013714, https://doi.org/10.1063/1.3676254.
[14] J.S. Ashwajeet, T. Sankarappa, R. Ramanna, T. Sujatha, A.M. Awasthi, Glass transition temperature and conductivity in Li2O and Na2O doped borophosphate glasses, in: AIP Conference Proceedings 1675, 020017, 2015, https://doi.org/10.1063/1.4929175.
[15] A. Marotta, A. Buri, F. Branda, P. Pernice, A. Aronne, Structure and devitrification behaviour of sodium, lithium and barium borophosphate glasses, Journal of Non-Crystalline Solids 95-96 (1987) 593–599, https://doi.org/10.1016/s0022-3093(87)80162-x.
[16] Stefan Elbers, Wenzel Strojek, Ladislav Koudelka, Hellmut Eckert, Site connectivity in silver borophosphate glasses: new results from 11B{31P} and 31P{11B} rotational echo double resonance NMR spectroscopy, Solid State Nuclear Magnetic Resonance 27 (1–2) (2005) 65–76, https://doi.org/10.1016/j.ssnmr.2004.08.007.
[17] A. Shaw, Arijit. Ghosh, Correlation of microscopic length scales of ion dynamics with network structure in lithium-iodide–doped lithium metaphosphate glasses, EPL (Europhysics Letters) 100 (2013) 66003, https://doi.org/10.1209/0295-5075/100/66003.
[18] B. Deb, A. Ghosh, Correlation of structure and dielectric properties of silver selenomolybdate glasses, J. Appl. Phys. 112 (2012), 024102, https://doi.org/10.1063/1.4737259.
[19] K.J. Hamam, F Salman, Dielectric constant and electrical study of solid-state electrolyte lithium phosphate glasses, Appl. Phys. A 125 (2019) 621, https://doi.org/10.1007/s00339-019-2868-2.
[20] NJ. Kim, SH. Im, DH. Kim, et al., Structure and properties of borophosphate glasses, Electron. Mater. Lett. 6 (2010) 103–106, https://doi.org/10.3365/eml.2010.09.103.
[21] P. Sharma, D.K. Kanchan, M. Pant, M.S. Jayswal, N. Gondaliya, Effect of AgI on Conduction Mechanism in Silver-Vanadate Superionic Glasses, New Journal of Glass and Ceramics 01 (03) (2011) 112–118, https://doi.org/10.4236/njgc.2011.13016.

[22] V.A. Adhwaryu, D.K. Kanchan, Ag+ ion conduction in AgI-Ag2O-B2O3-P2O5 glass electrolyte, Materials Science and Engineering: B 263 (2021), 114857, https://doi.org/10.1016/j.mseb.2020.114857. ISSN 0921-5107.
[23] D. Toloman, A.R. Biris, D. Maniu, I. Bratu, L.M. Giurgiu, A.S. Biris, I. Ardelean, Phosphate Glassy Network Depolymerization Induced by CaO Doping, Particulate Science and Technology, An International Journal 28 (3) (2010) 226–235, https://doi.org/10.1080/02726351.2010.481581.
[24] B.N. Nelson, Gregory J. Exarhos, Vibrational spectroscopy of cation-site interactions in phosphate glasses, J. Chem. Phys. 71 (1979) 2739, https://doi.org/10.1063/1.438679.
[25] Andrei M. Efimov, IR fundamental spectra and structure of pyrophosphate glasses along the 2ZnO•P2O5–2Me2O•P2O5 join (Me being Na and Li), Journal of Non-Crystalline Solids 209 (3) (1997) 209–226, https://doi.org/10.1016/S0022-3093(96)00562-5. ISSN 0022-3093.
[26] MyoLwin MyatHtut, Pho Kaung, Sein Htoon, Infrared Spectroscopic Study on the Structure of Ag2O.B2O3 Glasses, Jour. Myam Acad. Arts & Sc. IV (2) (2006).
[27] Ting Qiao Leow, Leong Ming, T. Eeu, Zuhairi Ibrahim, Rosli Hussin, Study of Structural and Luminescence Properties of Lead Lithium Borophosphate Glass System Doped with Ti Ions, SainsMalaysiana 43 (2014) 929–934.
[28] Ramdevudu Gokarakonda, L. Balachander, Dr Shareefuddin, Rodda Sayanna, Y. C. Venudhar, IR analysis of borate glasses containing three alkali oxides, Science Asia 39 (2013) 278, https://doi.org/10.2306/scienceasia1513-1874.2013.39.278.
[29] J.F. Ducel, J.J. Videau, Michel Couzi, Structural study of borophosphate glasses by Raman and infrared spectroscopy, Physics and Chemistry of Glasses 34 (1993) 212–218.
[30] Hatem A El-Batal, Zeinab S El-Mandouh, Hamdia A Zayed, Samir Y Marzouk, Gihan M El-Komy, Ahmed Hosny, Optical and infrared properties of lithium diborate glasses doped with copper oxide: Effect of gamma irradiation, Indian Journal of Pure & Applied Physics (IJPAP) 50 (06) (June 2012). http://nopr.niscair.res.in/handle/123456789/14182.
[31] Y.M. Lai, X.F. Liang, S.Y. Yang, J.X. Wang, L.H. Cao, B. Dai, Raman and FTIR spectra of iron phosphate glasses containing cerium, Journal of Molecular Structure 992 (1–3) (2011) 84–88, https://doi.org/10.1016/j.molstruc.2011.02.049. ISSN 0022-2860.
[32] Ming Wan, Poh Wong, Rosli Hussin, Zuhairi Ibrahim, Structural Study on Lithium-Barium Borophosphate Glasses Using Infrared and Raman Spectroscopy, Advanced Materials Research 626 (2012) 11–15, https://doi.org/10.4028/www.scientific.net/AMR.626.11.
[33] Chandkiram Gautam, Avadhesh Kumar Yadav, Arbind Kumar Singh, A Review on Infrared Spectroscopy of Borate Glasses with Effects of Different Additives, International Scholarly Research Notices 2012 (2012) 17, https://doi.org/10.5402/2012/428497. Article ID 428497.
[34] Daniela Carta, Dong Qiu, Paul Guerry, Ifty Ahmed, Ensanya A.Abou Neel, Jonathan C. Knowles, Mark E. Smith, Robert J. Newport, The effect of composition on the structure of sodium borophosphate glasses, Journal of Non-Crystalline Solids 354 (31) (2008) 3671–3677, https://doi.org/10.1016/j.jnoncrysol.2008.04.009. ISSN 0022-3093.
[35] James J. Hudgens, Steve W. Martin, Mid-IR and far-IR investigation of AgI-doped silver diborate glasses, Materials Science and Engineering Publications 66 (1996). https://lib.dr.iastate.edu/mse_pubs/66.
[36] H.A. Othman, H.S. Elkholy, I.Z. Hager, FTIR of binary lead borate glass: Structural investigation, Journal of Molecular Structure 1106 (2016) 286–290, https://doi.org/10.1016/j.molstruc.2015.10.076. ISSN 0022-2860.
[37] Rai, V. N., Raja Sekhar, B. N., Phase, D. M., and Deb, S. K., "Effect of gamma irradiation on the structure and valence state of Nd in phosphate glass", *arXiv e-prints*, 2014.
[38] S. Kabi, A. Ghosh, Mixed glass former effect in AgI doped silver borophosphate glasses, Solid State Ionics 262 (2014) 778–781, https://doi.org/10.1016/j.ssi.2013.09.028. ISSN 0167-2738.
[39] C A Angell, Mobile Ions in Amorphous Solids, Annual Review of Physical Chemistry 43 (1) (1992) 693–717, https://doi.org/10.1146/annurev.pc.43.100192.003401.
[40] Meenakshi Dult, R.S. Kundu, S. Murugavel, R. Punia, N. Kishore, Conduction mechanism in bismuth silicate glasses containing titanium, Physica B: Condensed Matter 452 (2014) 102–107, https://doi.org/10.1016/j.physb.2014.07.004. ISSN 0921-4526.
[41] Mohamed GABR, Karam Ali, Ahmed Mostafa, Infrared Analysis and Physical Properties Studies of B2O3 • CaO • ZnO • TiO2 Glass System, Turkish Journal of Physics (2007) 31.
[42] K.H. Mahmoud, F.M. Abdel-Rahim, K. Atef, Y.B. Saddeek, Dielectric dispersion in lithium–bismuth-borate glasses, Current Applied Physics 1 (11) (2011) 55–60, https://doi.org/10.1016/j.cap.2010.06.018. ISSN 1567-1739.
[43] F.H. Abd El-kader, A.M. shehap, M.S. Abo Ellil, K.H. Mahmoud, J. Polym. Mater 22 (2005) 349.
[44] Venkateswara Penugonda, Srinivasa Reddy, Maddireddy Kumar, V. Yerramreddy, Gandhi, Nalluri Veeraiah, Dielectric dispersion in PbO-Bi2O3-B 2O3 glasses mixed with TiO2, Turkish Journal of Physics 32 (2008).
[45] A Radoń, D Łukowiec, M Kremzer, J Mikuła, P. Włodarczyk, Electrical Conduction Mechanism and Dielectric Properties of Spherical Shaped Fe_3O_4 Nanoparticles Synthesized by Co-Precipitation Method, Materials (Basel) 11 (5) (2018 May 5) 735, https://doi.org/10.3390/ma11050735. PMID: 29734732; PMCID: PMC5978112.
[46] H. Jain, J.N. Mundy, Analysis of ac conductivity of glasses by a power law relationship, Journal of Non-Crystalline Solids 91 (3) (1987) 315–323, https://doi.org/10.1016/S0022-3093(87)80342-3. ISSN 0022-3093.
[47] A.R. Long, Frequency-dependent loss in amorphous semiconductors, Advances in Physics 31 (5) (1982) 553–637, https://doi.org/10.1080/00018738200101418.
[48] A. Ghosh, Transport properties of vanadium germanate glassy semiconductors, Phys. Rev. B 42 (9) (Sept 1990) 5665–5676, https://doi.org/10.1103/PhysRevB.42.5665.
[49] M. Pollak, On the frequency dependence of conductivity in amorphous solids, The Philosophical Magazine: A Journal of Theoretical Experimental and Applied Physics 23 (183) (1971) 519–542, https://doi.org/10.1080/14786437108216402.
[50] R. Punia, R.S. Kundu, Meenakshi Dult, S. Murugavel, N. Kishore, Temperature and frequency dependent conductivity of bismuth zinc vanadate semiconducting glassy system, Journal of Applied Physics 112 (2012), 083701, https://doi.org/10.1063/1.4759356.
[51] Manisha Paly, K. Segay, B.K. Chaudhuriz, H. Sakatay, Transport and dielectric properties of V2O5–MnO–TeO2 glasses, Philosophical Magazine 83 (11) (2003) 1379–1391.
[52] S.E. Anderson, R.S. Drago, The CBH model was introduced by Pike to account for the dielectric loss in scandium oxide, Physical Review B 6 (1972) 1527.
[53] S.R. Elliott, A.C. conduction in amorphous chalcogenide and pnictide semiconductors, Advances in Physics 36 (2) (1987) 135–217, https://doi.org/10.1080/00018738700101971.
[54] Jiji Koshy, Soosen Samuel, M.Anoop Chandran, K.C. George, Journal of Semiconductors Vol. 36 (12) (2015) s 122003-1 to 6.